Mekanika: Majalah Ilmiah Mekanika

Effect of Boundary Condition on Numerical Study of UAV Composite Skin Panels Under Dynamic Impact Loading

Ilham Bagus Wiranto[1], Sherly Octavia Saraswati[1], Iqbal Reza Alfikri[1], Chairunnisa[2], Fadli Cahya Megawanto[3], Muhammad Ilham Adhynugraha[3*], Nur Cholis Majid[4]

1 Research Center for Process and Manufacturing Industry Technology, BRIN, Banten, 15314, Indonesia
2 Research Center for Energy Conversion and Conservation, BRIN, Banten 15314, Indonesia
3 Research Center for Aeronautics Technology, BRIN, Bogor 16350, Indonesia
4 Department of Mechanical Engineering, King Abdulaziz University, Jeddah, Kingdom of Saudi Arabia

*Corresponding Author's email address: muha104@brin.go.id

Keywords:
Composites materials
Finite element analyses
Dynamic impact loading
Boundary condition

Abstract
In this study, a dynamic impact loading using Finite Element Analyses (FEA) was applied to an Unmanned Aerial Vehicle (UAV) composite skin panel. Two types of boundary condition panels were investigated (Fixed and Pinned). The composite UAV skin panel consists of upper panel and stiffener which have a thickness of 3 mm and 2 mm, respectively. The material properties used in this study was referring to Hexcel W3G282-F593 technical data sheet. A hemispherical steel indenter with 70 mm diameter and 120 kg of mass was used to crush the panel with a velocity of 4.43 m/s. The finite element analyses were performed using dynamic explicit solver in ABAQUS 6.23. At the beginning of study, the mesh convergence study was conducted to choose the proper mesh for main analysis. The convergence study was simulated using 20 kg mass to shorten computational time. The mesh size of 10 mm was chosen for the main analysis due to convergent result and short computational time compared to others mesh size. The impact deformation, contact force-displacement plot, and contact force-time plot was used to show the differences of using those boundary condition. The results show that fixed and pinned boundary condition reaches its contact force peak with the value of 29.2 kN and 22.8 kN, respectively.

1 Introduction

Composite material is a material that has remarkable specific strength, stiffness, and other physical qualities, and is starting to be commonly used in the world of transportation. Especially in Eurofighter and other advanced aircraft, the use of composites reaches almost 70% [1]. Composites are gaining popularity in the aircraft industry due to their higher strength-to-weight ratios and greater production feasibility for complicated components, distinctive shapes, and specific features [2-4]. To take advantage of the benefits of composite materials, metal components were replaced with composite materials in elements of the in-house project, specifically the Medium Altitude Long Endurance (MALE) project, particularly the wing and fuselage structures. Primarily, the composite replacement is aimed at lightening the weight of the MALE.

https://dx.doi.org/10.20961/mekanika.v23i1.77875

Revised 11 February 2024; received in revised version 28 February 2024; Accepted 10 March 2024
Available Online 29` March 2024

2579-3144

Aribowo et al. conducted optimization research on the male fuselage structure using the finite element method, as a result, a lighter fuselage structure was obtained by reducing the shape of the structural frame in the form of holes but still considering the required structural strength [5]. Composite structures are frequently formed of laminates with variable fiber orientation angles, generating unique results and ideal composite structural designs [6], and by integrating other materials. Adding various materials also contributes to boosting structural strength and stiffness [7-10]. Foam, honeycomb, and wood are common forms of cores utilized in aircraft applications. As a result, the mix of reinforcement, matrix (resins), and core systems results in laminate that can either enhance or deteriorate the constituent material qualities [11]. As a consequence of these combinations, it was necessary to create a laminate of stacking plies of multiple layer composites to understand structural behaviour with distinct orientations, as shown in Figure 1.

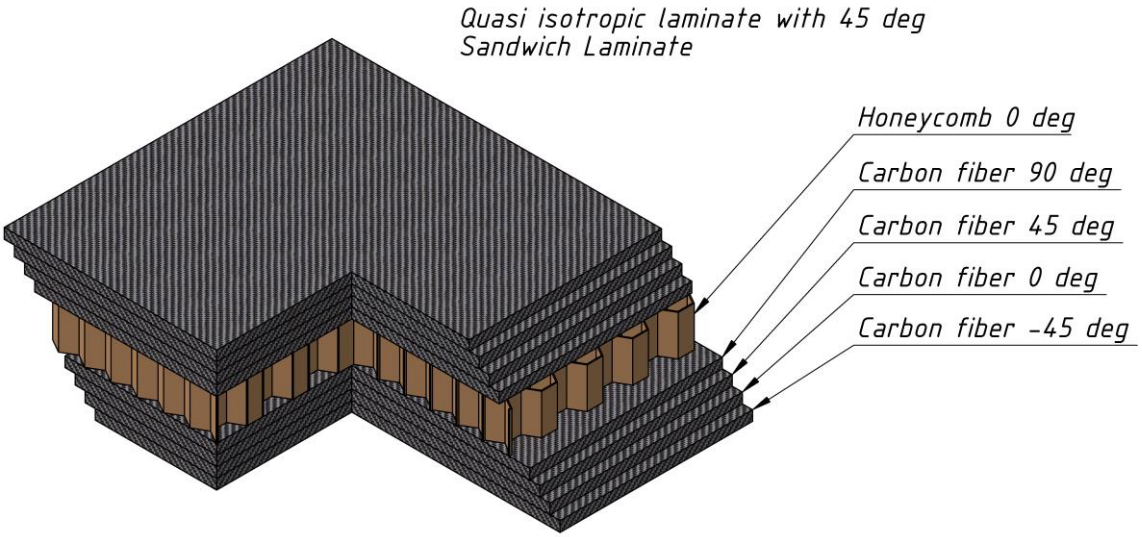

Figure 1. Composite laminate structure [8]

The arrangement of the components in the MALE fuselage is closely linked by connections. Many diverse types of connections are necessary, such as one between the skin and the bulkhead, the bulkhead and the deck, and the bulkhead and the stringer [5]. The work by Bautista et al. [12] sought to characterize these adhesive junctions when they were subjected to typical loads. To that end, an evaluation of the effects of adhesive thickness on the mechanical performances of such joints was carried out utilizing quasi-static loading conditions and impact fatigue, with Single Lap-Joint (SLJ) specimens. The dynamic analysis of composite structures is currently gaining greater focus, and many excellent theories on the finite element method for composite structural analysis have become provided [13].

The development of predictive computational models for the analysis and design of many complex engineering systems necessitates not only an accurate representation of relevant physics and their interactions, but also a quantitative assessment of underlying variability and its impact on design performance objectives [14]. Because experimental testing may reliably determine the properties of composites [15] the mixed numerical experimental technique is used to extract the physical information of composites. Typically, this entails minimizing an error function between experimental and numerical outputs [14]. As a result, extensive characterization of the mechanical properties of these structures is required in order to develop dependable designs.

In the discipline of aerospace engineering, structural analysis using the finite element method is known to be a particularly successful numerical simulation and optimization tool. Previous studies on finite element analysis have been provided in terms of software utilized and the results of the analyses undertaken, which span the scope of UAV wing [6]. Specifically, the finite element approach of numerical solutions applied to abstract calculus equations can be used to forecast the behaviour of physical systems under

external effects of any product design's structure [16]. Crashworthiness investigation of carbon fiber reinforced polymer composite structures filled with PU foam was conducted by Sabaey et al. as shown in Figure 2 [17]. The IM10 drop-weight impact machine was utilized. The striker mass and the total impactor mass (*m*) including the striker were 4 kg and 11.58 kg, respectively. Furthermore, the initial impact height (*h*) was 660 mm.

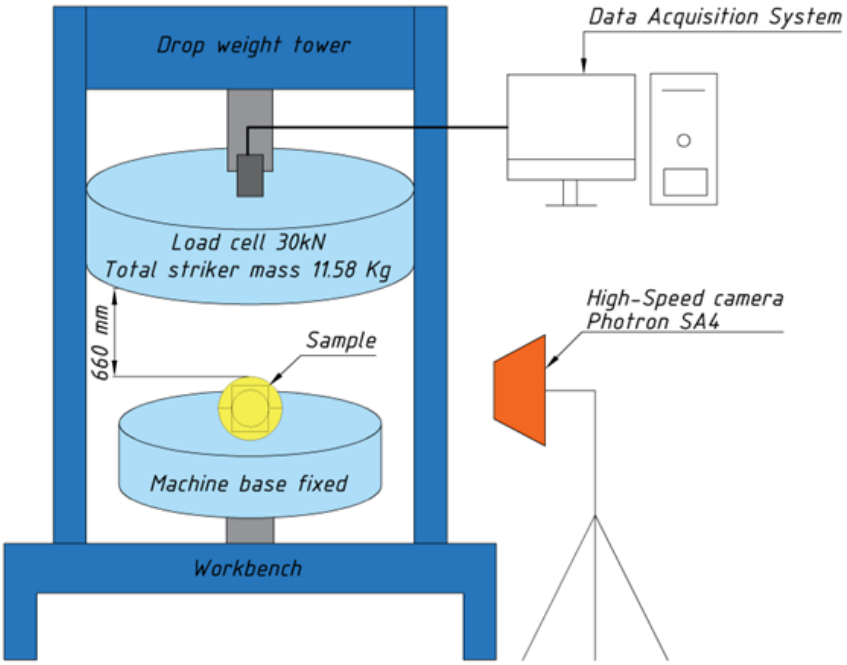

Figure 2. Drop weight impact test equipment and specimen [17]

There are several similar studies that have been carried out regarding drop tests. The impact test was carried out using a drop-hammer testing machine with a hammer weight of 77.89 kg. Desired results to get behaviour below quasi-static loading [18]. Impact characteristics of a thin flat plate to achieve the results seen in viscoelastically prestressed polymer matrix composite using projectile, a 532.9 g stainless steel ball with a diameter of 50.8 mm was used. The impact process, impact, and rebound kinetic energy are affected by projectile velocity and voltage [19]. The tests are carried out in an Instron 9450 drop tower testing equipment, which allows for the use of various impact masses, velocities, and energy up to 1800 J showing the effect of two parameters on the energy absorption of composite materials: specimen-to-anti-buckling fixture friction and crash velocity [20].

In this paper, two types of boundary condition during dynamic impact loading of UAV composite skin panel were investigated. The effect from using those boundary condition will be compared by force vs displacement diagram. Moreover, the damage visualization caused by those type of boundary condition is also presented. The composite panel was modelled using ABAQUS 6.23. methodological approaches utilized in this study to simulate dynamic impact loading are discussed.

2 Numerical Methods

Figure 3 shows the flow chart of numerical study of UAV composite skin panel under dynamic loading. The process starts with literature review to benchmark with previous study and define material properties for this study. Finite Element Method (FEM) model was constructed within ABAQUS. Mesh convergence study was conducted to choose the proper mesh size for main analysis where five different mesh sizes were investigated. If the model does not converge, then the mesh size is modified. The effect of two different boundary condition during axial impact loading of UAV composite panel were investigated for main analysis. Finally, the process ends with the data collection which shows the comparison between two different boundary condition.

2.1 Materials

The performance of composites is determined by the mechanical characteristics of each component. The interfacial connection between the matrix and fiber also affects the mechanical properties of composite materials. The composite skin panel are made of carbon fiber reinforced polymer consist of upper skin and stringer with the thickness of 3 mm and 2 mm, respectively. The mechanical properties of carbon fiber are shown in Table 1.

Table 1. Composite material properties for upper skin and stringer

Material	**Density (ton/mm^3)**	E_{11} **(MPa)**	E_{22} **(MPa)**	ν_{12} **(-)**	G_{12} **(MPa)**	G_{13} **(MPa)**	G_{23} **(MPa)**
Hexcel W3G282-F593 [21]	1.6×10^{-9}	55,840	55,840	0.06	3,650	3,650	3,650

Note: Thickness per ply 0.237 mm

The material modelling is done using ABAQUS. Firstly, the material properties for one layer of woven carbon fiber are input into a composite layup section and stacked until meeting the desired thickness. After that, ABAQUS will automatically generate a homogenous material for the analysis. Consequently, all layers have been formed as isotropic materials which makes this analysis more robust. A hemispherical indenter made of mild steel was used as an indenter in the experimental study. When modelling in ABAQUS, the indenter was assumed as a discrete rigid body which was used in contact analyses to model bodies that cannot deform. Furthermore, the mass should be defined within the simulation and set to have a weight of 120 kg.

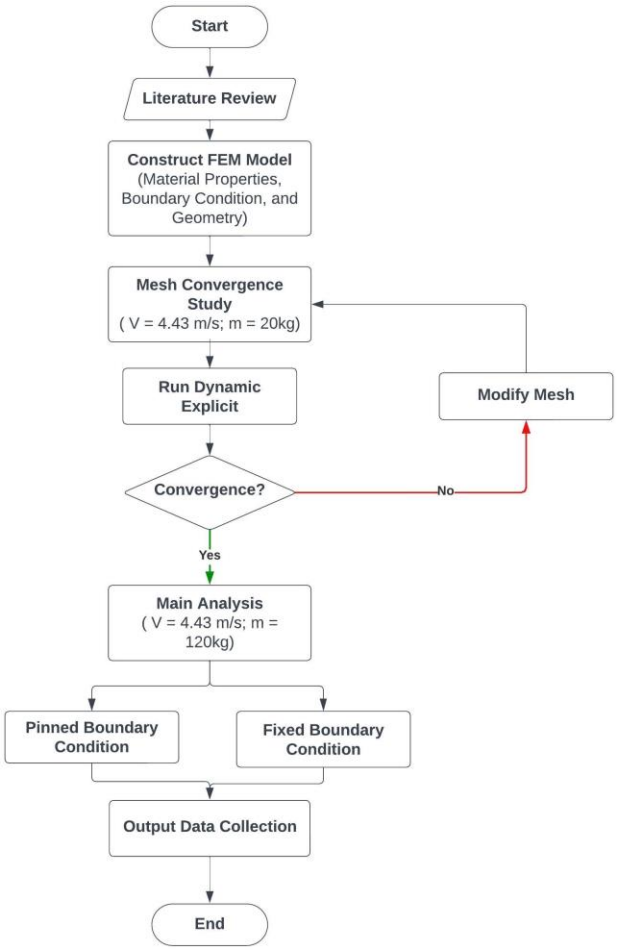

Figure 3. Research workflow

2.2 Numerical setup

The finite element analysis was performed using dynamic explicit in ABAQUS 6.23 [22]. Firstly, the model was created using ABAQUS, the upper skin, and stringer were modelled as one part and defined as deformable shell elements. As for the indenter, it was modelled as a discrete rigid body which means the bodies cannot deform during impact. Before performing the analysis, the mesh convergence study was conducted. The mesh convergence analysis was performed by changing the mesh size. The optimum mesh size was chosen based on result convergencies and total running time. Furthermore, In the simulation environment, the indenter, specimen, and rigid support facility (boundary condition) were taken into account. To ensure simulation accuracy and calculation efficiency, a simplified model was created. In this analysis, the boundary conditions are varied using fixed and pinned conditions. Figure 4 shows the geometry and boundary condition within the simulation.

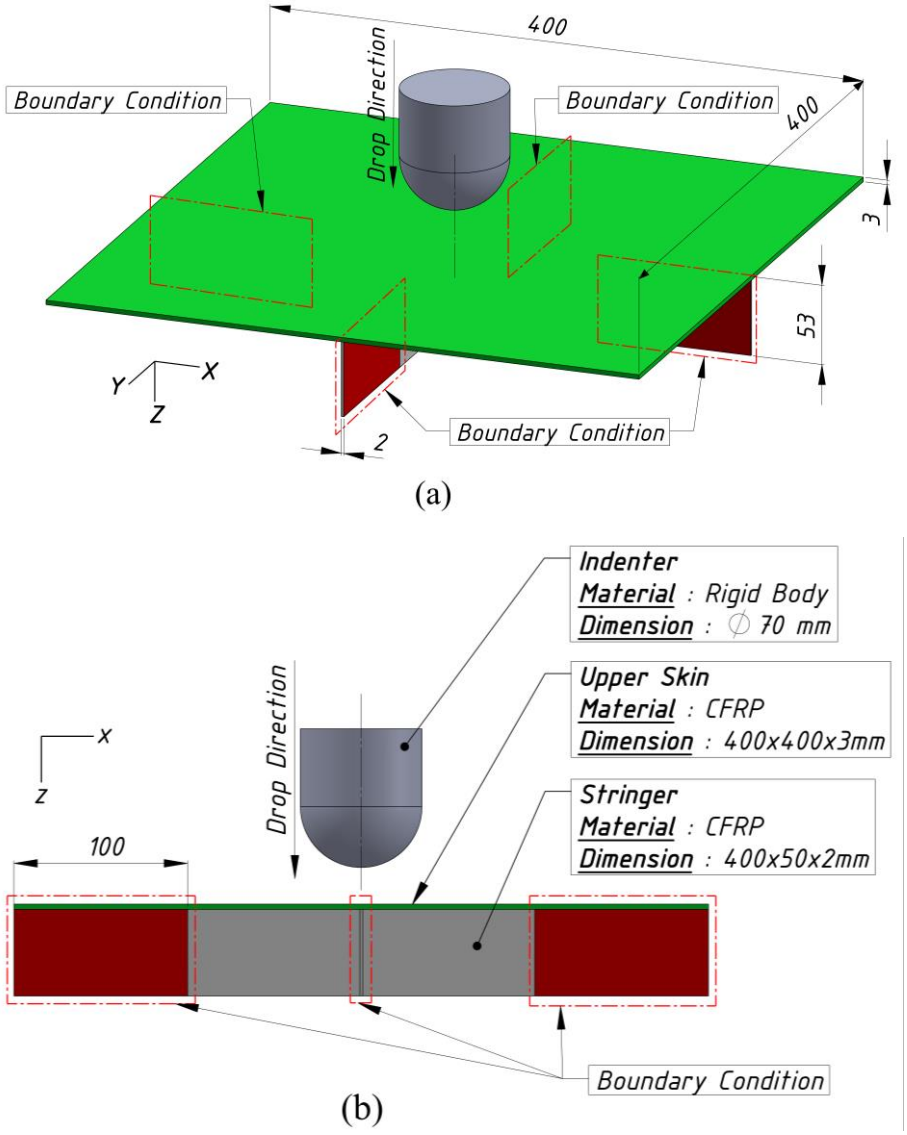

Figure 4. Geometry and boundary condition of composite panel and indenter

In the simulation, the indenter was assumed to drop from 1m of height with 120 kg of mass. The indenter was set to hit the center of the panel. Furthermore, to simplify the simulation, the boundary condition was applied to the indenter which makes the indenter only have a displacement in Z-axis. The indenter needs an initial velocity as input to move along the axis, consequently, 4.43 m/s was set to the simulation which represents the speed drop from 1 m of height to generate total impact energy of 1 kJ.

3 Results and Discussion

The outcomes of the numerical simulations described in the previous section are examined and compared in this section. Firstly, this study begins with mesh convergence analysis to verify the proper mesh size for the model. The mesh was assigned as a uniform mesh with a size of 5, 10, 15, 20, 25, and 30 which has a total element of 8000, 2000, 952, 520, 320, and 120, respectively. In order to shorten the computing time, the mass used in convergence studies was 20 kg. The convergence test results are shown in Figure 5.

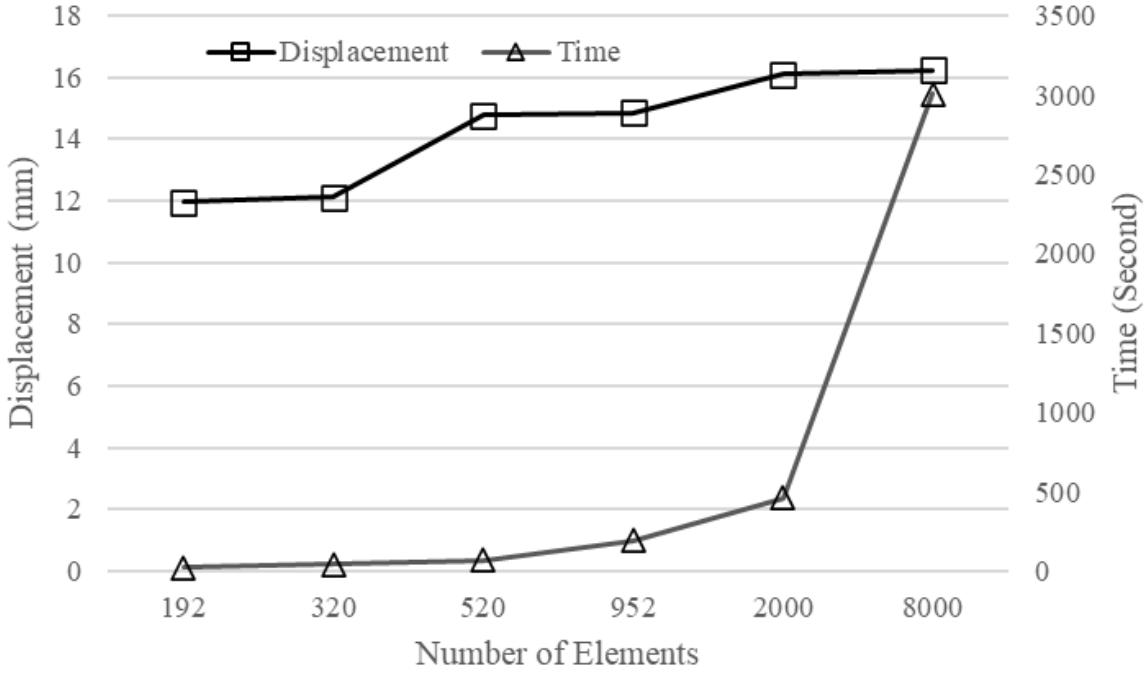

Figure 5. Mesh convergence analysis result

The displacement value starts to converge when the mesh size of 10 and 5 were utilized. However, the computing time increased drastically to almost 3000 s when running the smallest mesh size. Based on this investigation, the selected mesh size for the main analysis was 10 x10 mm with total elements of 2000 as shown in Figure 6.

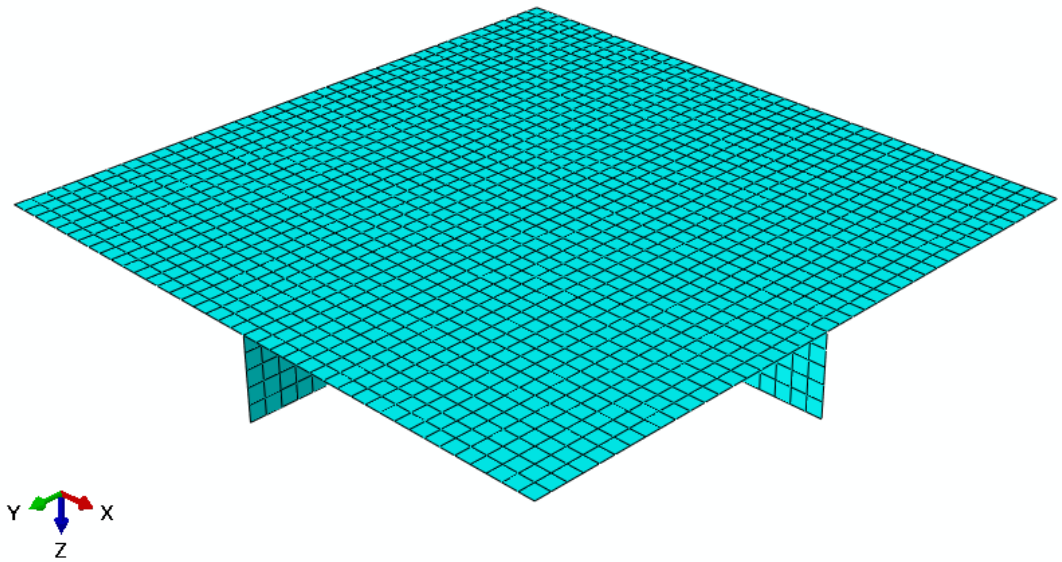

Figure 6. Detail of mesh size 10 x 10 mm with 2000 elements

The dynamic explicit simulation has been done in ABAQUS with the variation of boundary condition. The deformation results between fixed and pinned condition are depicted in Figure 7 and Figure 8. The maximum values of deformation between fixed and pinned condition are 56.794 mm and 58.7175 mm, respectively. The displacement of fixed boundary condition is relatively smaller than pinned condition, since a fixed boundary condition restricts all six Degree of Freedoms (DOFs-three translations and three rotations) of a node. Moreover, it can be seen in pinned boundary condition the upper skin and the stringer experienced a larger deflection area, this can happen because in pinned boundary condition only restricts the translational DOFs (three translations) of a node while allowing rotations.

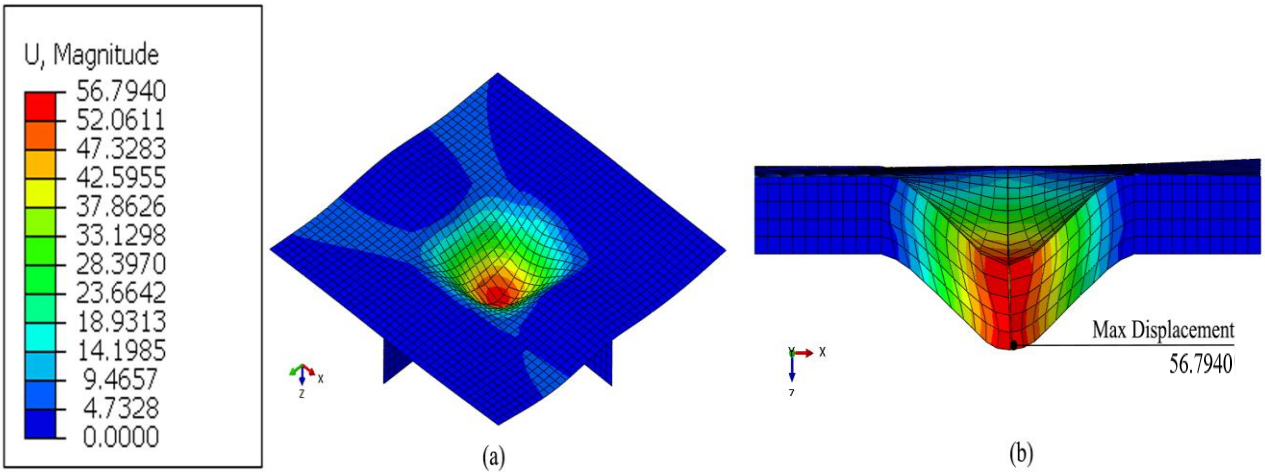

Figure 7. Deformation at maximum displacement of fixed condition: (a) Isometric-view and (b) Side-view

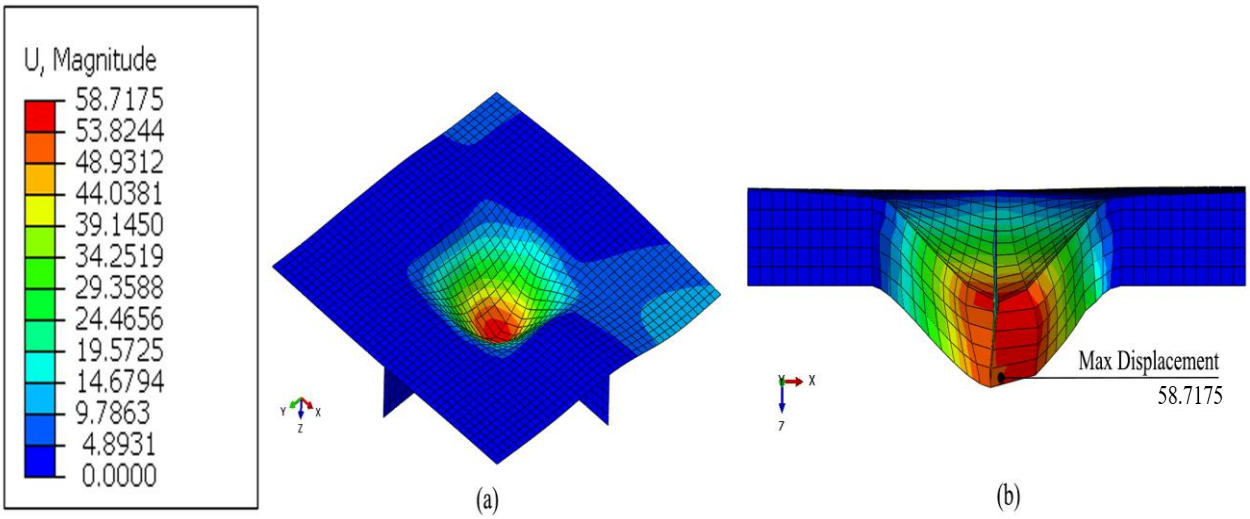

Figure 8. Deformation at maximum displacement of pinned condition: (a) Isometric-view and (b) Side-view

The simulation of drop test impact results in the form of contact force-displacement and contact force-time are plotted in Figures 9 and 10. In Figure 9, when the force value returns to zero, the corresponding displacement of the impactor remains finitely positive, indicating that the impactor and the specimens lost contact before the impactor returned to its original position at the start of impact. There are two reasons regarding this phenomenon. First, when a matrix crack opens, the fibers contained within the matrix may stick into the crack and prevent the crack from fully closing up, which is one of the factors that may be causing this residual displacement. Second, residual strain is thus produced because the matrix itself during the impact may experience plastic deformation.

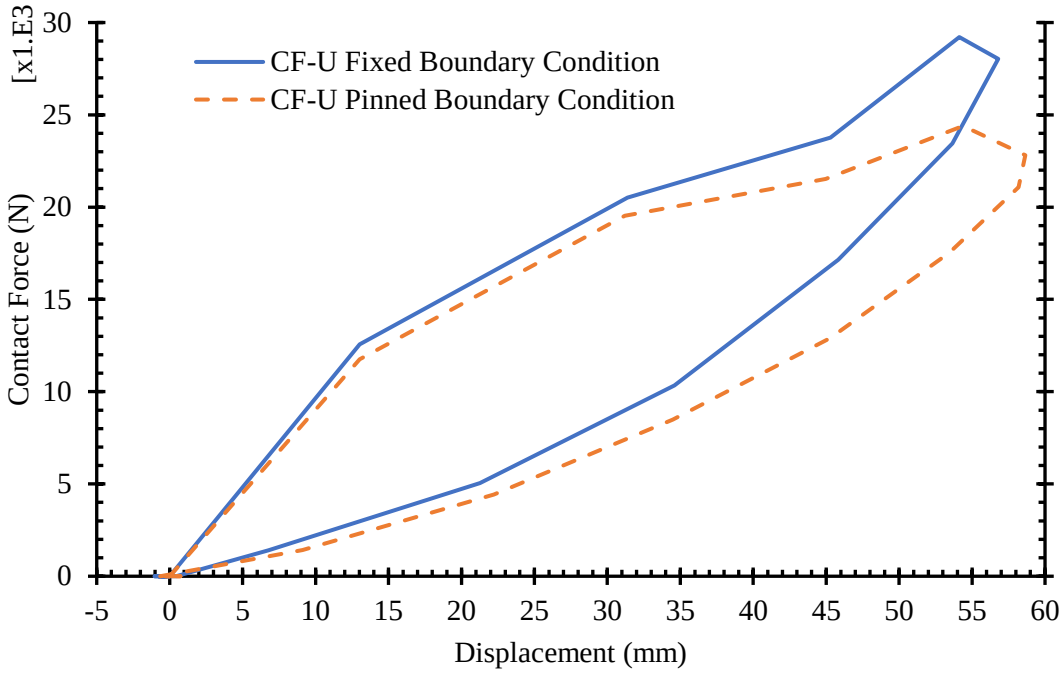

Figure 9. Contact Force – Displacements response of fixed and pinned boundary condition

In Figure 10, a total time recorded for this simulation is limited to 0.1 s. It can be seen at the beginning of simulation there is no contact force, indicating the impactor has not touched the specimen since the impactor is located 10 mm above the specimen. Furthermore, at 0.02 s the impactor for fixed and pinned boundary condition reaches its contact force peak with the value of 29.2 kN and 22.8 kN, respectively. This indicates that there is an initial failure in the specimen shortly after the impactor strikes the specimen [23]. Finally, there is no contact anymore between impactor and specimen after 0.055 s for fixed condition and 0.6 s for pinned condition.

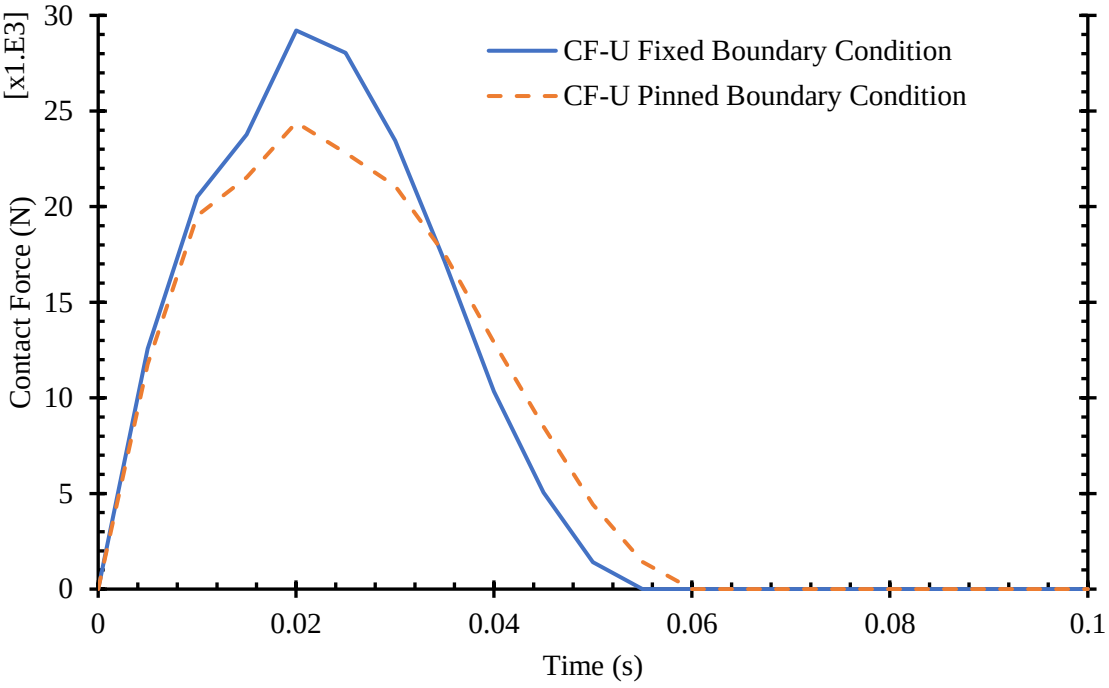

Figure 10. Contact force – time response

Figure 11 shows the damage dissipation energy diagram as a function of time for pinned and fixed boundary conditions, when the impactor positioned 10 mm above the specimen. Damage dissipation energy is used in the context of materials or structures, it typically refers to the amount of energy that is absorbed and dissipated by a material during the process of damage or deformation. Higher damage dissipation energy implies that the material has a greater capacity to absorb and dissipate energy when subjected to external forces, impacts, or other forms of stress. In this scenario, the increased freedom can sometimes result in higher dissipation of energy during dynamic events, for example choosing pinned boundary condition.

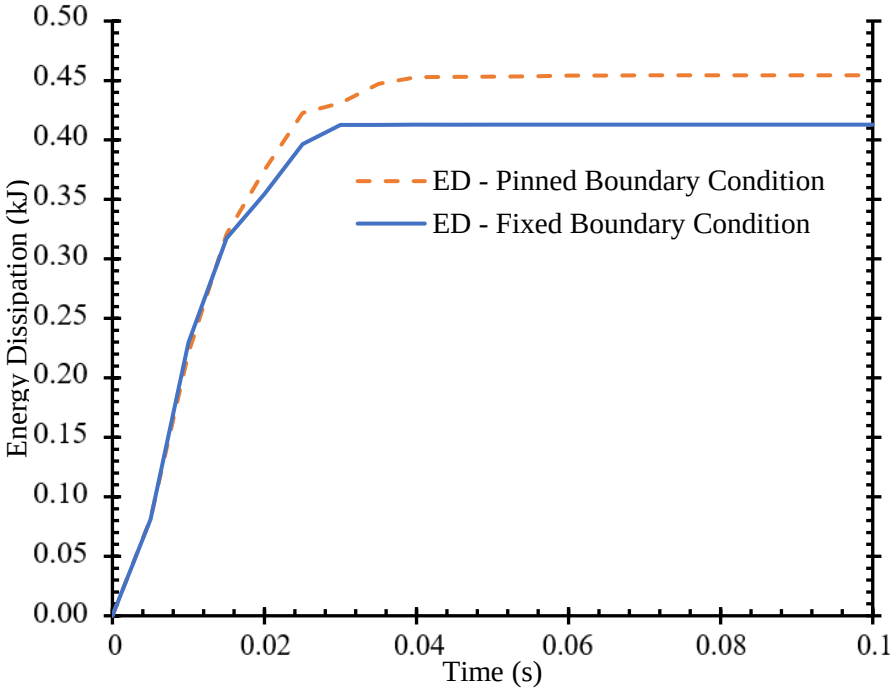

Figure 11. Damage dissipation energy – time response

The graph represents a gradual increase in energy dissipation as time goes by and tends to stabilize after 0.04 seconds for pinned and fixed boundary conditions. The trend line of the energy dissipation has a similar with previous study [24]. Especially, the energy dissipation begins to undergo a change after 0.015 seconds for both the pinned and fixed boundary conditions. This indicates the beginning of the occurrence of failure. Specifically, under pinned boundary conditions, the total energy dissipation present values approximately 10.064% higher than those observed under fixed boundary conditions. When the impactor strikes the specimen, there is a possibility that the specimen may shift, leading to suboptimal contact between the impactor and the specimen's surface. As a result of the pinned boundary condition, which allow for more freedom of movement compared to the fixed boundary conditions.

4 Conclusions

A numerical study on axial impact loading of UAV composite skin panel using FEM has been developed. The simulation was investigated the effect of boundary condition used during axial impact loading simulation. The mesh convergence study is conducted to choose the proper mesh before running the main analysis. Six different mesh size was investigated and it was found that a mesh size of 10 was considered the best for this model. The UAV skin panel structure’s material properties are assumed made from composite laminate material from HexPly W3G282-F593 carbon fiber prepreg. The load used in this study is a combination of impactor mass and velocity during impact loading. Impactor mass during mesh convergence study and main analysis are 20 kg and 120 kg, respectively. The velocity for both analyses was assign to 4.43 m/s. For the main analysis, it was found that fixed and pinned boundary condition reaches its contact force peak with the value of 29.2 kN and 22.8 kN, respectively. The pinned boundary condition

resulted around 10% higher than fixed boundary condition in terms of damage dissipation energy. Appropriate boundary condition representation is essential to obtaining results from finite element simulations that are comprehensible and trustworthy. The unique behaviour and constraints of the actual structure being modelled should be taken into consideration while choosing the boundary conditions. It is crucial to take into account the structure's real support characteristics and applied loads. In some circumstances, it may be necessary to combine fixed and pinned boundary condition in order to correctly simulate the actual constraints and produce useful simulation results.

5 Acknowledgements

This work is part of the research scope of Numerical Testing and Validation of Crashworthiness Analysis in Composite Fuselage Design of Unmanned Aerial Vehicle (UAV) in collaboration with the Department of Mechanical Engineering Universitas Sebelas Maret, Surakarta, supported by The Nanotechnology and Materials Research Organization BRIN through the Fundamental Molecular Science Research Program 2023.

References

1. National Research Council, *Going to extremes: Meeting the emerging demand for durable polymer matrix composites*, Washington D.C.: National Academies Press, 2005.
2. S. D. Salman, Z. Leman, M. T. H. Sultan, M. R. Ishak, and F. Cardona, “Effect of kenaf fibers on trauma penetration depth and ballistic impact resistance for laminated composites,” *Text. Res. J.*, vol. 87, no. 17, pp. 2051-2065, 2017.
3. A. U. M. Shah, M. T. H. Sultan, F. Cardona, M. Jawaid, and N. Yidris, “Thermal analysis of bamboo fibre and its composites,” *BioResources*, vol. 12 no. 2, pp. 2394-2406, 2017.
4. N. H. Mostafa, Z. N. Ismarrubie, S. M. Sapuan, and M. T. H. Sultan, “Fibre prestressed composites: Theoretical and numerical modelling of unidirectional and plain-weave fibre reinforcement forms,” *Compos. Struct.*, vol. 159, pp. 410-423, 2017.
5. A. Aribowo, M. I. Adhynugraha, F. C. Megawanto, A. Hidayat, T. Muttaqie, F. A. Wandono, A. Nurrohmad, Chairunnisa, S. O. Saraswati, I. B. Wiranto, I. R. Al Fikri, and M. D. Saputra, “Finite element method on topology optimization applied to laminate composite of fuselage structure,” *Curved Layer. Struct.*, vol. 10, no. 1, article no. 20220191, 2023.
6. E. I. Basri, M. T. Sultan, M. Faizal, A. A. Basri, M. F. Abas, M. A. Majid, J. S. Mandeep, and K. A. Ahmad, “Performance analysis of composite ply orientation in aeronautical application of unmanned aerial vehicle (UAV) NACA4415 wing,” *J. Mater. Res. Technol.*, vol. 8, no. 5, pp. 3822-3834, 2019.
7. A. Nagesh, *Comparative Analysis of the Structural Properties of Materials Tested Under Fatigue Stresses Used in the Fuselage of an Airplane, and to Thereby Determine the Fuselage Materials Efficiency*, Pennsylvania: Pennsylvania State University, 2017.
8. N. H. Mostafa, Z. N. Ismarrubie, S. M. Sapuan, and M. T. H. Sultan, “Effect of equi-biaxially fabric prestressing on the tensile performance of woven E-glass/polyester reinforced composites,” *J. Reinf. Plast. Compos.*, vol. 35, no. 14, pp. 1093-1103, 2016.
9. S. D. Salman, M. J. Sharba, Z. Leman, M. T. Sultan, M. R. Ishak, and F. Cardona, “Tension-compression fatigue behavior of plain woven kenaf/kevlar hybrid composites,” *BioResources*, vol. 11, no. 2, pp. 3575-3586, 2016.
10. S. D. Salman, Z. Leman, M. T. H. Sultan, M. R. Ishak, and F. Cardona, “Influence of fiber content on mechanical and morphological properties of woven kenaf reinforced PVB film produced using a hot press technique,” *Int. J. Polym. Sci.*, 2016.
11. W. D. Callister, *Materials Science and Engineering: An Introduction*, 7th ed. New Jersey: John Wiley & Sons, Inc., 2007.
12. A. Bautista, J. P. Casas-Rodriguez, M. Silva, and A. Porras, “A dynamic response analysis of adhesive-Bonded single lap joints used in military aircrafts made of glass fiber composite material undercyclic impact loading,” *Int. J. Adhes.*, vol. 102, article no. 102644, 2020.
13. G. Georgiou, A. Manan, and J. E. Cooper, “Modeling composite wing aeroelastic behavior with uncertain damage severity and material properties,” *Mech. Syst. Signal. Process.*, vol. 32, pp. 32-43, 2012.
14. L. Mehrez, A. Doostan, D. Moens, and D. Vandepitte, “Stochastic identification of composite material

properties from limited experimental databases, Part II: Uncertainty modelling," *Mech. Syst. Signal. Process.*, vol. 27, pp. 484-498, 2012.
15. D. Jiang, Y. Li, Q. Fei, and S. Wu, "Prediction of uncertain elastic parameters of a braided composite," *Compos. Struct.*, vol. 126, pp. 123-131 2015.
16. F. Mehta, H. Joshi, "Finite element method: An overview," *IOSR J. Dent. Med. Sci.*, vol. 15, no. 3, pp. 38-41, 2016.
17. T. A. Sebaey, D. K. Rajak, and H. Mehboob, "Internally stiffened foam-filled carbon fiber reinforced composite tubes under impact loading for energy absorption applications," *Compos. Struct.*, vol. 255, article no. 112910, 2021.
18. Z. Huang, X. Zhang, and C. Yang, "Static and dynamic axial crushing of Al/CRFP hybrid tubes with single-cell and multi-cell sections," *Compos. Struct.*, vol. 226, article no. 111023, 2019.
19. Y. Qin, and K. S. Fancey, "Drop weight impact behaviour of viscoelastically prestressed composites," *Compos. Part A Appl. Sci. Manuf.*, vol. 131, article no. 105782, 2020.
20. L. Vigna, A. Calzolari, G. Galizia, G. Belingardi, and D. S. Paolino, "Effect of impact speed and friction on the in-plane crashworthiness of composite plates," *Procedia Struct. Integr.*, vol. 33, pp. 623-629, 2021.
21. Hexcel Corporation, *HexPly F593 Product Datasheet*, Stamford: Hexcel Corporation, 2020.
22. ABAQUS, *Analysis User's Manual, Version 6.23*, California: ABAQUS Inc., 2023.
23. M. A. Abd El-baky, D. A. Hegazy, and M. A. Hassan, "Novel energy absorbent composites for crashworthiness applications," *J. Ind. Text.*, vol. 51, pp. 6403S-6442S, 2022.
24. P. W. Chen, and Y. Y. Lin, "Evaluation on crashworthiness and energy absorption of composite light airplane," *Adv. Mech. Eng.*, vol. 10, no. 8, article no. 1687814018794080, 2018.